

$[\text{H}_2\text{bpy}]_2[\{\text{Cu}(\text{btepy})_2\}\text{Mo}_5\text{P}_2\text{O}_{23}]\cdot 4\text{H}_2\text{O}$: A Three-Dimensional Framework Built from Transition-Metal Coordination Polymer Sheets Pillared by Polyoxomolybdophosphate Clusters

Ying Lu,^[a] Yangguang Li,^[a,b] Enbo Wang,^{*[a]} Jian Lü,^[a] Lin Xu,^[a] and Rodolphe Clérac^{*[b]}

Keywords: Coordination polymers / Magnetic properties / Hydrothermal synthesis / Polyoxometallates

$[\text{H}_2\text{bpy}]_2[\{\text{Cu}(\text{bpy})_2\}\text{Mo}_5\text{P}_2\text{O}_{23}]\cdot 4\text{H}_2\text{O}$ (**1**; bpy = 4,4'-bipyridine) contains the first three-dimensional framework based on two-dimensional transition metal coordination polymer sheets pillared by polyoxomolybdophosphate clusters. It crystallises in the *C2/c* monoclinic space group with $a = 17.630(4)$ Å, $b = 13.670(3)$ Å, $c = 25.111(5)$ Å, and $\beta = 106.61(3)^\circ$. Thermogravimetric analysis shows that guest

molecules (H_2O and free bpy ligands) can be easily removed from **1** by simple heat treatment without losing the three-dimensional framework. Moreover, the paramagnetic properties of the $\{\text{Cu}(\text{bpy})_2\}$ arrays, make this material an interesting magnetic solid based on polyoxometallate clusters.

(© Wiley-VCH Verlag GmbH & Co. KGaA, 69451 Weinheim, Germany, 2005)

Introduction

Porous materials have attracted much attention due to their potential applications in gas storage, ion exchange or heterogeneous catalysis.^[1] A promising approach toward the synthesis of these porous materials is the design of metal-organic frameworks built from transition metal ions and bridging organic ligands.^[2] In this field, the synthesis of robust three-dimensional (3D) frameworks with high porosity and thermal stability has become an important issue.^[3] Pillared-layer structures have been proven to be an effective route to design 3D frameworks with large channels. In the known pillared-layer structure, bidentate linear organic ligands such as 4,4'-bipyridine, pyrazine and 1,2-bis(4-pyridyl)ethylene play the role of pillars.^[4] An alternative choice of pillars may be the polyoxometallate (POM) clusters. Indeed, the occupation of their surface by oxygen atoms offers the possibility of coordination to other transition metals^[5] and hence their use as pillars to link transition metal coordination polymer sheets. In addition, POMs possess interesting properties, for example in catalysis, magnetism and nonlinear optics,^[6] and also have a higher thermal stability than organic ligands, which may strengthen the

thermal stability of the pillared-layer structures formed. Hence, the combination of POMs and transition metal coordination polymer appears to be an appealing route to design multifunctional porous hybrid materials. Unfortunately, this strategy remains unexplored due to the difficulties in combining appropriate POM clusters and 2D transition metal coordination polymer networks while controlling their interactions to form a three-dimensional architecture.

Among the possible POMs, polyoxomolybdophosphate clusters of general formula, $[\text{H}_x\text{Mo}_5\text{P}_2\text{O}_{23}]^{(6-x)-}$ ($x = 0, 1, 2$)^[7] have recently proved their ability to form organic-inorganic hybrid materials through their coordination to transition-metal complexes.^[5c,8] Although the number of organic-inorganic hybrid materials based on these clusters is limited in the literature, $[\text{H}_x\text{Mo}_5\text{P}_2\text{O}_{23}]^{(6-x)-}$ clusters can be regarded as valuable building units due to their ability to link transition-metal complexes in diverse coordination modes^[5c,8] and their chemical versatility – they can easily be modified at the molecular level by substitution of phosphate groups by organophosphate functions.^[9] In our quest for the right polyoxometallate cluster to assemble two dimensional arrays into 3D porous materials, $[\text{H}_x\text{Mo}_5\text{P}_2\text{O}_{23}]^{(6-x)-}$ clusters appeared to be good candidates. This idea was reinforced by the chemistry of these clusters, which can be easily performed under hydrothermal conditions by mixing Na_2MoO_4 (or MoO_3) and H_3PO_4 in water; they are also stable over a wide pH range (3–6).

We report here the novel compound $[\text{H}_2\text{bpy}]_2[\{\text{Cu}(\text{bpy})_2\}\text{Mo}_5\text{P}_2\text{O}_{23}]\cdot 4\text{H}_2\text{O}$ (**1**; bpy = 4,4'-bipyridine) which exhibits a 3D framework of 1D channels built from $\{\text{Cu}(\text{bpy})_2\}_n^{2n+}$ coordination polymer sheets pillared by $[\text{Mo}_5\text{P}_2\text{O}_{23}]^{6-}$ clusters.

[a] Institute of Polyoxometallate Chemistry, Department of Chemistry, Northeast Normal University, Changchun, 130024, P. R. China
Fax: +86-431-509-8787
E-mail: wangenbo@public.cc.jl.cn

[b] Centre de Recherche Paul Pascal, CNRS UPR 8641, 115 Avenue du Dr. A. Schweitzer, 33600 Pessac, France
Fax: +33-556-855-600

E-mail: clerac@crpp-bordeaux.cnrs.fr

Supporting information for this article is available on the WWW under <http://www.eurjic.org> or from the author.

Results and Discussion

Synthesis

The successful isolation of compound **1** depends on the exploitation of hydrothermal techniques. Hydrothermal synthesis has recently been proved to be a particularly useful technique in the preparation of inorganic–organic hybrid materials.^[10] In the hydrothermal environment, the reduced viscosity of the solvent results in enhanced rates of solvent extraction of solids and crystal growth from solution. Furthermore, since different solubility problems can be minimised, a variety of organic and inorganic precursors can be introduced. However, hydrothermal synthesis is still a relatively complex process because many factors can influence the outcome of reaction, such as the type of initial reactants, starting concentrations, pH values, reaction time and temperature.^[11]

Compound **1** was separated from the hydrothermal reaction of $\text{Na}_2\text{MoO}_4 \cdot 2\text{H}_2\text{O}$, H_3PO_4 , $\text{Cu}(\text{MeCO}_2)_2 \cdot \text{H}_2\text{O}$, 4,4'-bpy and water in the molar ratio of 4:4:1:1:550 at 160 °C for six days. Parallel experiments showed that the pH value of the reaction system is crucial for the crystallisation of compound **1**: blue crystals of compound **1** could only be obtained in the pH range 4–5. At pH 3–4 no crystalline phase was formed and the products were a mixture of blue and white powders. However, at lower pH (2.5–3) another novel compound reported by our group could be synthesised, which shows a two dimensional structure constructed from interconnecting polyoxomolybdate chains $\{\text{HPCuMo}_{11}\text{O}_{39}\}_n^{4n-}$ and transition metal coordination polymer chains $\{\text{Cu}(\text{bpy})\}_n^{n+}$.^[5a] In addition, the nature of

the divalent transition metal is crucial for the formation of the pillared-layer structure of compound **1**. We tried to replace $\text{Cu}(\text{MeCO}_2)_2 \cdot \text{H}_2\text{O}$ with $\text{Co}(\text{MeCO}_2)_2 \cdot 4\text{H}_2\text{O}$, $\text{Ni}(\text{MeCO}_2)_2 \cdot 4\text{H}_2\text{O}$ or $\text{Zn}(\text{MeCO}_2)_2 \cdot 2\text{H}_2\text{O}$ in the synthesis of compound **1**, but no isostructural compounds were obtained.

Crystal Structure

A single-crystal X-ray diffraction analysis was performed on **1**; the basic motif of the structure is shown in Figure 1. The $[\text{Mo}_5\text{P}_2\text{O}_{23}]^{6-}$ cluster can be described as a ring of five distorted MoO_6 octahedra with two capped PO_4 tetrahedra on each side. Each phosphate subunit shares three oxo groups with the molybdate ring. One of these oxo-groups (O8) adopts a μ_2 -bridging mode, linking Mo1 to P1, and the two others (O2 and O6) adopt a μ_3 -bridging mode, linking Mo2, Mo3 (or Mo1) and the P1 site. The fourth oxygen (O3) of the PO_4 is dangling. The Cu1 site adopts a “4+2” axially distorted geometry, characteristic of a d^9 Jahn–Teller distortion.^[8b,12] Its equatorial and axial positions are occupied by four nitrogen donors from the four distinct bpy ligands and two oxo groups (O5) from adjacent $[\text{Mo}_5\text{P}_2\text{O}_{23}]^{6-}$ clusters, respectively. The Cu–N and Cu–O bond lengths are 2.062 Å (Cu1–N1), 2.041 Å (Cu1–N2) and 2.423 Å (Cu1–O5).

The three-dimensional structure of **1** is composed of square-grid $\{\text{Cu}(\text{bpy})_2\}_n^{2n+}$ layers pillared by $[\text{Mo}_5\text{P}_2\text{O}_{23}]^{6-}$ clusters. The $\{\text{Cu}(\text{bpy})_2\}_n^{2n+}$ layers lie parallel to the *ab* plane (Figure 2). Each layer consists of a square lattice of Cu^{II} and bpy located at the corners and the edges, respec-

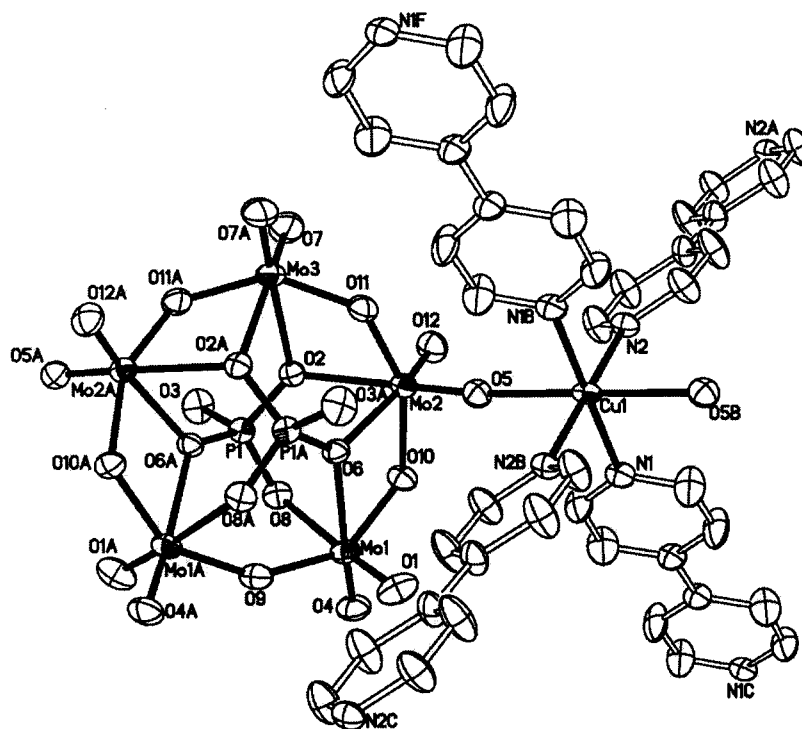


Figure 1. ORTEP drawing of the basic crystallographic unit in **1**. All the hydrogen atoms, $\text{H}_2\text{bpy}^{2+}$ and H_2O have been omitted for clarity.

tively. As observed in related materials,^[13] this type of arrangement leads to a square cavity of about $11.2 \times 11.2 \text{ \AA}^2$. Moreover, it is noteworthy that the layers are perfectly planar with the equatorial plane of the Cu coordination sphere. Adjacent square-grid layers are connected by $[\text{Mo}_5\text{P}_2\text{O}_{23}]^{6-}$ clusters through the axial positions of the Cu site to form the 3D open framework (Figure 3). This organisation leads to the formation of channels in two directions: along the *c* axis the channels have an elliptical shape of about $11.2 \times 6.5 \text{ \AA}^2$ (Figure 4) and along the *b* axis rectangular channels can be observed with dimensions of about $10.0 \times 3.7 \text{ \AA}^2$. Free bipyridine and H_2O molecules are located in these channels. According to the consideration of the charge balance and weak acidic conditions of the synthesis, the free bipyridines are doubly protonated.

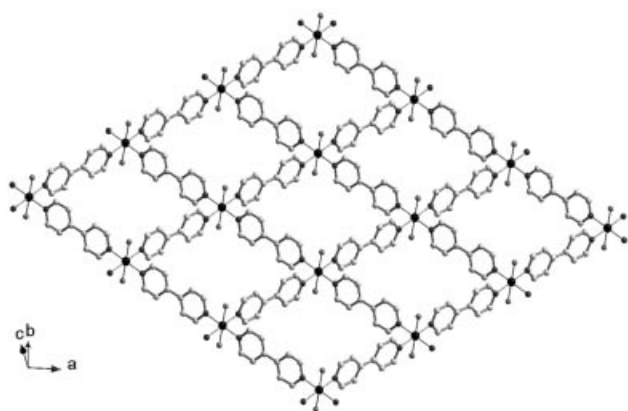


Figure 2. View of the 2D square-grid layer in **1**.

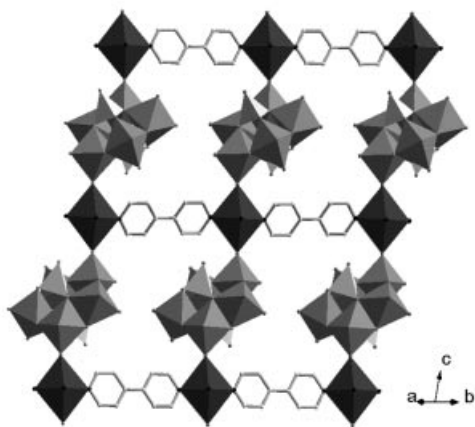


Figure 3. Polyhedral representation of the 3D network in **1**. Guest molecules included in the channels have been omitted for clarity.

Thermogravimetric analysis (TGA) was performed in air at a heating rate of $10 \text{ }^\circ\text{C min}^{-1}$ on a polycrystalline sample of **1** (Figure 5). A first weight loss of 4.4% occurred between 40 and $150 \text{ }^\circ\text{C}$, corresponding to the loss of four water molecules (calcd. 4.3%). In the range $240\text{--}340 \text{ }^\circ\text{C}$, a second weight loss of 18.6% is observed corresponding to the loss of two free bpy molecules (calcd. 18.8%). Between 390 and $610 \text{ }^\circ\text{C}$ a weight loss of 19.5% is due to loss of the

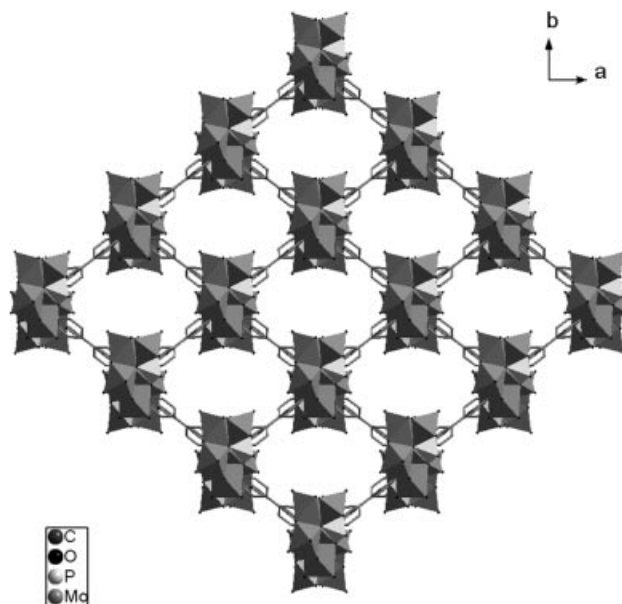


Figure 4. View of the 3D network along the *c* axis. Guest molecules included in the channels have been omitted for clarity.

coordinated bpy ligands. Above $610 \text{ }^\circ\text{C}$ and up to $750 \text{ }^\circ\text{C}$ no further weight loss is observed. Over the whole range of temperature explored, the total weight loss (42.5%) agrees well with the calculated value (41.8%). The final product was found to be amorphous by powder X-ray diffraction.

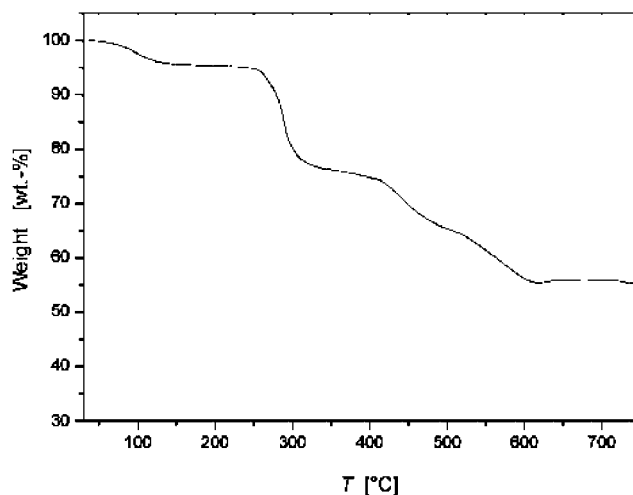


Figure 5. Thermogravimetric analysis curve of **1**.

Based on the TG analysis, **1** was heated in air at $350 \text{ }^\circ\text{C}$ for six hours to remove the free bpy ligands and water molecules and form **1'**. The elemental analysis of **1'** (C 18.9, H 1.5, N 4.6) agrees well with the expected formula for the opened $[\text{H}_4\{\text{Cu}(\text{bpy})_2\}\text{Mo}_5\text{P}_2\text{O}_{23}]$ network (calcd. C 18.6, H 1.6, N 4.3). The TG curve of **1'** also confirms that water molecules and free bpy ligands have been removed (Supporting Information, Figure S1). The X-ray powder diffraction spectra of **1** and **1'** (Figure S2) were compared and found to be very similar, thereby confirming that the framework of **1** is retained after the loss of the guest molecules.

This phenomenon, where a compound retains its framework structure after guest organoamine molecules have been removed, has been reported by several groups.^[14]

Magnetic Properties

The magnetic susceptibility of **1** was studied from 300 K to 1.83 K at 1000 Oe on a polycrystalline sample. The χT vs. T plot, shown in Figure 6, decreases continuously from 0.42 cm³ K mol⁻¹ at 300 K to reach 0.24 cm³ K mol⁻¹ at 1.83 K. Based on the structure analysis, the spins are carried by the Cu^{II} centres, which are organized into well-separated, 2D square arrays. Therefore, the magnetic susceptibility was analysed using an $S = 1/2$ Heisenberg 2D square lattice model. A high temperature series-expansion for the susceptibility of this model has been reported by Rushbrooke and Wood.^[15a] To fit the experimental data, the compact expression of Lines^[15b] was used, with the following spin Hamiltonian:

$$H = -2J \sum_{\langle i,j \rangle} S_i S_j$$

$$\frac{Ng^2\mu_B^2}{2\chi J} = 3\theta + \sum_{n=1}^6 \frac{C_n}{\theta^{n-1}}$$

where $\theta = k_B T / [2J]S(S+1)$, $C_1 = 4$, $C_2 = 2.667$, $C_3 = 1.185$, $C_4 = 0.149$, $C_5 = -0.191$, $C_6 = 0.001$ and N , g , and μ_B have their usual meanings. The best set of parameters are $J/k_B = -0.53(1)$ K and $g = 2.11(1)$. The fitting procedure was performed down to 1.83 K as the validity condition $k_B T \approx 0.9JS(S+1)$ for this model was not reached.^[15b] The J value obtained confirms that the interaction through the bridging bpy is weak, in agreement with the large Cu–Cu distance (ca. 11.2 Å).

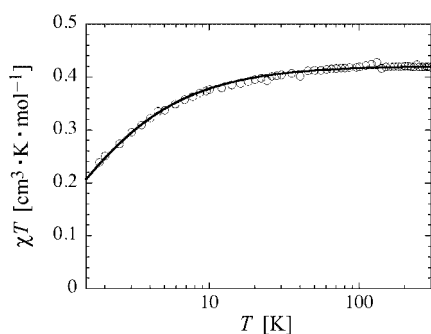


Figure 6. Temperature dependence of the χT product measured at 1000 Oe in the temperature range 1.83–300 K. The solid line is the best fit obtained with the $S = 1/2$ Heisenberg two-dimensional anti-ferromagnetic square lattice model.^[15]

The room-temperature EPR spectrum of **1** (Supporting Information, Figure S3) shows a typical Cu²⁺ signal in an elongated octahedral coordination geometry, as expected from the crystal structure. The eigenvalues of the g tensor can be calculated as $g_{\parallel} = 2.1538(1)$ and $g_{\perp} = 2.0539(1)$; they are in relatively good agreement with the average value ($g = 2.11$) found by susceptibility measurements.

Conclusion

In summary, we have reported here the first 3D structure based on a transition-metal coordination polymer sheet linked by polyoxomolybdo-phosphate clusters. The successful synthesis of **1** provides an interesting illustration of the use of polyoxometallate clusters to obtain new magnetic materials. Since chemical modifications of the polyoxometallate cluster and the transition-metal coordination polymer sheet may be easily achieved, a complete new family of magnetic solids should be accessible in the near future.

Experimental Section

Materials and General Methods: Reagents were purchased commercially and used without further purification. Elemental analyses (C, H and N) were performed on a Perkin–Elmer 2400 CHN Elemental Analyzer. Mo, Cu and P were determined with a Leeman inductively coupled plasma (ICP) spectrometer. The IR spectrum was obtained on an Alpha Centaur FT/IR spectrometer with pressed KBr pellet in the 4000–400 cm⁻¹ regions. A Perkin–Elmer TGA7 thermogravimetric analyzer was used to obtain TGA curves under N₂ with a temperature increasing rate of 10 °C min⁻¹. X-ray powder diffraction (XRPD) patterns were recorded on a Siemens D5005 diffractometer with Cu- K_{α} ($\lambda = 1.5418$ Å) radiation. The EPR spectrum was recorded on a Bruker ER 200D spectrometer at room temperature. The magnetic susceptibility data were measured with a Quantum Design SQUID magnetometer MPMS-XL.

Synthesis of 1: In a typical synthesis of compound **1**, Cu(MeCO₂)₂·H₂O (1 mmol) and 4,4'-bpy (1 mmol) were added to a stirred solution of Na₂MoO₄·2H₂O (4 mmol) and H₃PO₄ (4 mmol) in water (10 mL). The resultant mixture was sealed in a 23-mL, Teflon-lined autoclave and heated at 160 °C for 6 d. The initial pH value of the reaction solution was ca. 4.6 and the final pH value was ca. 5.5. Blue, block-like crystals of **1** were obtained from the solid product in a yield of 60% (0.65 g) with respect to 4,4'-bpy. C₄₀H₄₄CuMo₅N₈O₂₇P₂ (1674.0): calcd. C 28.70, H 2.65, Cu 3.80, Mo 28.66, N 6.69, P 3.70; found C 28.58, H 2.59, Cu 3.67, Mo 28.81, N 6.65, P 3.62. IR (KBr pellet): $\tilde{\nu} = 3448$ (s), 3100 (w), 1607

Table 1. Crystal data and structure refinement for **1**.

Empirical formula	C ₄₀ H ₄₄ CuMo ₅ N ₈ O ₂₇ P ₂
Formula mass	1673.97
Temperature [K]	293(2)
Wavelength [Å]	0.71073
Crystal system	monoclinic
Space group	C2/c
<i>a</i> [Å]	17.630(4)
<i>b</i> [Å]	13.670(3)
<i>c</i> [Å]	25.111(5)
β [°]	106.61(3)
<i>V</i> [Å ³]	5799(2)
<i>Z</i>	4
<i>D</i> _{calcd.} [g cm ⁻³]	1.912
μ [mm ⁻¹]	1.553
<i>F</i> ₀₀₀	3280
Data/restraints/parameters	6582/158/516
Goodness-of-fit on <i>F</i> ²	1.039
<i>R</i> ₁ ^[a] [<i>I</i> > 2σ(<i>I</i>)]	0.0555
<i>wR</i> ₂ ^[b]	0.1365
Largest diff. peak and hole [e·Å ⁻³]	0.680 and -0.978

[a] $R_1 = \Sigma ||F_o| - |F_c|| / \Sigma |F_o|$. [b] $wR_2 = \Sigma [w(F_o^2 - F_c^2)^2] / \Sigma [w(F_o^2)^2]^{1/2}$.

(m), 1535 (w), 1512 (w), 1488 (w), 1411 (w), 1126 (m), 1066 (w), 1032 (m), 1012 (m), 914 (vs), 884 (s), 827 (w), 803 (w), 700 (vs), 671 (vs), 558 (m) cm^{-1} (see Supporting Information, Figure S4).

X-ray Crystallography: A blue single crystal of **1** was carefully selected under a polarizing microscope and glued to the tip of a thin glass fibre with cyanoacrylate (super glue) adhesive. Single-crystal structure determination by X-ray diffraction was performed on an R-axis RAPID IP diffractometer equipped with a normal focus, 18 kW sealed tube X-ray source (Mo- K_{α} radiation, $\lambda = 0.71073 \text{ \AA}$) operating at 50 kV and 200 mA. Data processing was accomplished with the RAXWISH processing program.^[16] An empirical absorp-

tion correction was applied. The structure was solved by direct methods and refined by full-matrix least-squares on F^2 using the SHELXL 97 software.^[17] All the non-hydrogen atoms were refined anisotropically. The hydrogen atoms were located from difference Fourier maps. Further details of the X-ray structural analysis are given in Table 1. Selected bond lengths and angles are listed in Table 2.

CCDC-239758 contains the supplementary crystallographic data for this paper. These data can be obtained free of charge from The Cambridge Crystallographic Data Centre via www.ccdc.cam.ac.uk/data_request/cif.

Supporting Information Available (see also footnote on the first page of this article): The TG curve of **1'**, the XRPD patterns for **1** and **1'**, IR and ESR spectra for **1**, space-filling diagram of the three-dimensional framework of **1** and a view of the 3D network of **1** along the b axis.

Acknowledgment

The authors thank the National Natural Science Foundation of China (20371011) for financial support.

Table 2. Bond lengths [\AA] and angles [$^{\circ}$] for **1**.^[a]

Mo(1)–O(4)	1.713(4)	Mo(1)–O(1)	1.723(5)
Mo(1)–O(9)	1.8990(18)	Mo(1)–O(10)	1.938(4)
Mo(1)–O(8)	2.279(4)	Mo(1)–O(6)	2.367(4)
Mo(2)–O(12)	1.697(4)	Mo(2)–O(5)	1.740(4)
Mo(2)–O(11)	1.905(4)	Mo(2)–O(10)	1.960(4)
Mo(2)–O(6)	2.214(4)	Mo(2)–O(2)	2.353(4)
Mo(3)–O(7)#1	1.714(5)	Mo(3)–O(7)	1.714(5)
Mo(3)–O(11)#1	1.916(4)	Mo(3)–O(11)	1.916(4)
Mo(3)–O(2)	2.362(4)	Mo(3)–O(2)#1	2.362(4)
Cu(1)–N(2)	2.041(5)	Cu(1)–N(2)#2	2.041(5)
Cu(1)–N(1)#2	2.062(5)	Cu(1)–N(1)	2.062(5)
Cu(1)–O(5)#2	2.423(4)	Cu(1)–O(5)	2.423(4)
P(1)–O(8)	1.509(4)	P(1)–O(6)#1	1.536(4)
P(1)–O(2)	1.547(4)	P(1)–O(3)	1.574(4)
O(4)–Mo(1)–O(1)	102.7(2)	O(4)–Mo(1)–O(9)	102.4(2)
O(1)–Mo(1)–O(9)	98.7(2)	O(4)–Mo(1)–O(10)	99.8(2)
O(1)–Mo(1)–O(10)	101.5(2)	O(9)–Mo(1)–O(10)	145.8(2)
O(4)–Mo(1)–O(8)	84.1(2)	O(1)–Mo(1)–O(8)	173.2(2)
O(9)–Mo(1)–O(8)	79.94(15)	O(10)–Mo(1)–O(8)	76.80(17)
O(4)–Mo(1)–O(6)	167.65(19)	O(1)–Mo(1)–O(6)	86.2(2)
O(9)–Mo(1)–O(6)	84.50(18)	O(10)–Mo(1)–O(6)	69.65(15)
O(8)–Mo(1)–O(6)	87.05(14)	O(12)–Mo(2)–O(5)	104.8(2)
O(12)–Mo(2)–O(11)	101.2(2)	O(5)–Mo(2)–O(11)	95.94(19)
O(12)–Mo(2)–O(10)	96.4(2)	O(5)–Mo(2)–O(10)	98.96(19)
O(11)–Mo(2)–O(10)	153.13(18)	O(12)–Mo(2)–O(6)	159.87(19)
O(5)–Mo(2)–O(6)	93.75(17)	O(11)–Mo(2)–O(6)	84.14(17)
O(10)–Mo(2)–O(6)	72.73(16)	O(12)–Mo(2)–O(2)	89.44(19)
O(5)–Mo(2)–O(2)	163.61(17)	O(11)–Mo(2)–O(2)	72.99(17)
O(10)–Mo(2)–O(2)	87.18(16)	O(6)–Mo(2)–O(2)	73.46(14)
O(7)#1–Mo(3)–O(7)	104.2(4)	O(7)#1–Mo(3)–O(11)	102.3(2)
O(7)–Mo(3)–O(11)#1	98.9(2)	O(7)#1–Mo(3)–O(11)	98.9(2)
O(7)–Mo(3)–O(11)	102.3(2)	O(11)#1–Mo(3)–O(11)	145.2(3)
O(7)#1–Mo(3)–O(2)	166.4(2)	O(7)–Mo(3)–O(2)	88.2(2)
O(11)#1–Mo(3)–O(2)	80.87(17)	O(11)–Mo(3)–O(2)	72.58(16)
O(7)#1–Mo(3)–O(2)	88.2(2)	O(7)–Mo(3)–O(2)#1	166.4(2)
O(11)#1–Mo(3)–O(2)	72.58(16)	O(11)–Mo(3)–O(2)#1	80.87(17)
O(2)–Mo(3)–O(2)#1	80.05(19)	N(2)–Cu(1)–N(2)#2	180.0(3)
N(2)–Cu(1)–N(1)#2	92.50(19)	N(2)#2–Cu(1)–N(1)#2	87.50(19)
N(2)–Cu(1)–N(1)	87.50(19)	N(2)#2–Cu(1)–N(1)	92.50(19)
N(1)#2–Cu(1)–N(1)	180.0(3)	N(2)–Cu(1)–O(5)#2	92.63(17)
N(2)#2–Cu(1)–O(5)	87.37(17)	N(1)#2–Cu(1)–O(5)#2	87.58(17)
N(1)–Cu(1)–O(5)#2	92.42(17)	N(2)–Cu(1)–O(5)	87.37(17)
N(2)#2–Cu(1)–O(5)	92.63(17)	N(1)#2–Cu(1)–O(5)	92.42(17)
N(1)–Cu(1)–O(5)	87.58(17)	O(5)#2–Cu(1)–O(5)	180.0(2)
O(8)–P(1)–O(6)#1	108.6(2)	O(8)–P(1)–O(2)	111.5(2)
O(6)#1–P(1)–O(2)	110.5(2)	O(8)–P(1)–O(3)	110.8(3)
O(6)#1–P(1)–O(3)	105.9(2)	O(2)–P(1)–O(3)	109.3(3)
P(1)–O(2)–Mo(2)	127.9(2)	P(1)–O(2)–Mo(3)	126.7(2)
Mo(2)–O(2)–Mo(3)	91.01(14)	Mo(2)–O(5)–Cu(1)	174.7(2)
P(1)#1–O(6)–Mo(2)	129.7(2)	P(1)#1–O(6)–Mo(1)	133.4(2)
Mo(2)–O(6)–Mo(1)	95.80(14)	P(1)–O(8)–Mo(1)	120.6(2)
Mo(1)–O(9)–Mo(1)#1	148.1(4)	Mo(1)–O(10)–Mo(2)	121.5(2)
Mo(2)–O(11)–Mo(3)	123.3(2)		

[a] Symmetry transformations used to generate equivalent atoms: #1: $-x, y, -z + 1/2$; #2: $-x, -y, -z$.

- [1] a) K. Biradha, Y. Hongo, M. Fujita, *Angew. Chem. Int. Ed.* **2000**, *39*, 3843–3845; b) B. Moulton, M. J. Zaworotko, *Chem. Rev.* **2001**, *101*, 1629–1658; c) M. Eddaoudi, D. B. Moler, H. L. Li, B. L. Chen, T. M. Reineke, M. O'Keeffe, O. M. Yaghi, *Acc. Chem. Res.* **2001**, *34*, 319–330; d) U. Kortz, S. S. Hamzeh, N. A. Nasser, *Chem. Eur. J.* **2003**, *9*, 2945–2952; e) C. N. R. Rao, S. Natarajan, R. Vaidhyanathan, *Angew. Chem. Int. Ed.* **2004**, *43*, 1466–1496.
- [2] a) S. S.-Y. Chui, S. M.-F. Lo, J. P. H. Charmant, A. G. Orpen, I. D. Williams, *Science* **1999**, *283*, 1148–1150; b) S. Kitagawa, R. Kikawa, S.-I. Noro, *Angew. Chem. Int. Ed.* **2004**, *43*, 2334–2375; c) Y.-Q. Tian, C.-X. Cai, X.-M. Ren, C.-Y. Duan, Y. Xu, S. Gao, X. Z. You, *Chem. Eur. J.* **2003**, *9*, 5673–5685.
- [3] a) X.-H. Bu, M.-L. Tong, H.-C. Chang, S. Kitagawa, S. R. Batten, *Angew. Chem. Int. Ed.* **2004**, *43*, 192–195; b) C.-Y. Su, A. M. Goforth, M. D. Smith, P. J. Pellechia, H.-C. zur Loye, *J. Am. Chem. Soc.* **2004**, *126*, 3576–3586; c) B. Zhao, P. Cheng, X. Y. Chen, C. Cheng, W. Shi, D. Z. Liao, S. P. Yan, Z. H. Jiang, *J. Am. Chem. Soc.* **2004**, *126*, 3012–3013.
- [4] a) S. Subramanian, M. J. Zaworotko, *Angew. Chem. Int. Ed. Engl.* **1995**, *34*, 2127–2130; b) S.-I. Noro, S. Kitagawa, M. Kondo, K. Seki, *Angew. Chem. Int. Ed.* **2000**, *39*, 2081–2084; c) X. L. Wang, C. Qin, E. B. Wang, Y. Y. Li, C. W. Hu, L. Xu, *Chem. Commun.* **2004**, 378–379.
- [5] a) Y. Lu, Y. Xu, E. Wang, J. Lü, C. Hu, L. Xu, *Cryst. Growth Des.* **2004** in press; b) A. Dolbecq, P. Mialane, L. Lissard, J. Marrot, F. Sécheresse, *Chem. Eur. J.* **2003**, *9*, 2914–2920; c) J.-J. Lu, Y. Xu, N. K. Goh, L. S. Chia, *Chem. Commun.* **1998**, 2733–2734; d) C.-M. Liu, D.-Q. Zhang, M. Xiong, D.-B. Zhu, *Chem. Commun.* **2002**, 1416–1417; e) A. Tripathi, T. Hughbanks, A. Clearfield, *J. Am. Chem. Soc.* **2003**, *125*, 10 528–10 529; f) D. Hargman, J. Zubieta, *Chem. Commun.* **1998**, 2005–2006; g) U. Kortz, S. Matta, *Inorg. Chem.* **2001**, *40*, 815–817; h) J. R. Galán-Mascarós, C. Giménez-Saiz, S. Triki, C. J. Gómez-García, E. Coronado, L. Ouahab, *Angew. Chem. Int. Ed. Engl.* **1995**, *34*, 1460–1462.
- [6] D. E. Katsoulis, *Chem. Rev.* **1998**, *98*, 359–388.
- [7] a) R. Strandberg, *Acta Chem. Scand.* **1973**, *27*, 1004–1018; b) B. Hedman, *Acta Chem. Scand.* **1973**, *27*, 3335–3354.
- [8] a) J. Chen, S. F. Lu, R. M. Yu, Z. N. Chen, Z. X. Huang, C. Z. Lu, *Chem. Commun.* **2002**, 2640–2641; b) E. Burkholder, J. Zubieta, *Chem. Commun.* **2001**, 2056–2057.
- [9] a) U. Kortz, C. Marquer, R. Thouvenot, M. Nierlich, *Inorg. Chem.* **2003**, *42*, 1158–1162; b) R. C. Finn, E. Burkholder, J. Zubieta, *Chem. Commun.* **2001**, 1852–1853.

- [10] a) M. Yuan, Y. G. Li, E. B. Wang, C. G. Tian, L. Wang, C. W. Hu, N. H. Hu, H. Q. Jia, *Inorg. Chem.* **2003**, *42*, 3670–3676; b) D.-Q. Chu, J.-Q. Xu, L.-M. Duan, T.-G. Wang, A.-Q. Tang, L. Ye, *Eur. J. Inorg. Chem.* **2001**, 1135–1137.
- [11] P. J. Hagrman, D. Hagrman, J. Zubieta, *Angew. Chem. Int. Ed.* **1999**, *38*, 2638–2684.
- [12] a) V. Shivaiah, M. Nagaraju, S. K. Das, *Inorg. Chem.* **2003**, *42*, 6604–6606; b) C.-Z. Lu, C.-D. Wu, S.-F. Lu, J.-C. Liu, Q.-J. Wu, H.-H. Zhuang, J.-S. Huang, *Chem. Commun.* **2002**, 152–153.
- [13] a) M.-L. Tong, B.-H. Ye, J.-W. Cai, X.-M. Chen, S. W. Ng, *Inorg. Chem.* **1998**, *37*, 2645–2650; b) S. Kawata, S. Kitagawa, M. Kondo, I. Furuchi, M. Munakata, *Angew. Chem. Int. Ed. Engl.* **1994**, *33*, 1759–1761.
- [14] a) C.-H. Huang, L.-H. Huang, K.-H. Lii, *Inorg. Chem.* **2001**, *40*, 2625–2627; b) J. H. Lou, M. C. Hong, R. H. Wang, R. Cao, L. Han, D. Q. Yuan, Z. Z. Lin, Y. F. Zhou, *Inorg. Chem.* **2003**, *42*, 4486–4488; c) X.-M. Zhang, M.-L. Tong, M.-L. Gong, X.-M. Chen, *Eur. J. Inorg. Chem.* **2003**, 138–142.
- [15] a) G. S. Rushbrooke, P. J. Wood, *Mol. Phys.* **1958**, *1*, 257–283; b) M. E. Lines, *J. Phys. Chem. Solids* **1970**, *31*, 101–106; c) J. Darriet, M. S. Haddad, E. N. Duesler, D. N. Hendrickson, *Inorg. Chem.* **1979**, *18*, 2679–2682.
- [16] H. Uekusa, *J. Crystallogr. Soc. Jpn.* **1999**, *41*, 82–91.
- [17] G. M. Sheldrick, *SHELXS-97, Program for Crystal Structure Solution*, University of Göttingen, Germany, **1997**.

Received: September 06, 2004